

BiLSTM Multitask Learning-Based Combined Load Forecasting Considering the Loads Coupling Relationship for Multienergy System

Yixiu Guo, Yong Li[✉], Senior Member, IEEE, Xuebo Qiao, Student Member, IEEE, Zhenyu Zhang, Wangfeng Zhou, Yujie Mei, Jinjie Lin, Student Member, IEEE, Yicheng Zhou, Senior Member, IEEE, and Yosuke Nakanishi, Member, IEEE

Abstract—Accurate load forecasting is the key to economic dispatch and efficient operation of Multi-Energy System (MES). This paper proposes a combined load forecasting method for MES based on Bi-directional Long Short-Term Memory (BiLSTM) multi-task learning. Firstly, this paper investigates the multi-energy interaction mechanism and multi-loads characteristics and analyzes the correlation of multi-loads in different seasons. Then, a combined load forecasting method is proposed, which focuses on making full use of the coupling relationship among multiple loads. In the forecasting model, the different loads are selected combinedly as the input features according to the Maximum Information Coefficient (MIC). The multi-task learning is adopted to construct the cooling, heating and electric combined load forecasting model based on the BiLSTM algorithm, which can effectively share the coupling information among the loads. Finally, case studies verify the effectiveness and superiority of the proposed method in both learning speed and forecasting accuracy.

Index Terms—Multi-task learning, coupling relationship among loads, multi-energy system, combined load forecasting.

I. INTRODUCTION

IN RECENT years, the multi-energy system (MES) has become a research hotspot due to the advantages of flexible and efficient energy production and utilization [1]. Compared with the traditional independent energy system,

Manuscript received 29 August 2021; revised 1 January 2022; accepted 15 April 2022. Date of publication 10 May 2022; date of current version 23 August 2022. This work was supported in part by the International Science and Technology Cooperation Program of China under Grant 2018YFE0125300; in part by the National Natural Science Foundation of China under Grant 52061130217; in part by the Science and Technology Project of State Grid Hunan Electric Power Company Ltd. under Grant H202194400109; in part by the Innovative Construction Program of Hunan Province of China under Grant 2019RS1016; and in part by the Innovative Team Projects of Zhuhai City under Grant ZH01110405180049PWC. Paper no. TSG-01379-2021. (*Corresponding author: Yong Li*)

Yixiu Guo, Yong Li, Xuebo Qiao, Zhenyu Zhang, Wangfeng Zhou, Yujie Mei, and Jinjie Lin are with the College of Electrical and Information Engineering, Hunan University, Changsha 410082, China (e-mail: yixiuguo@hnu.edu.cn; yongli@hnu.edu.cn; xbq1992@hnu.edu.cn; zhenyuzhang@hnu.edu.cn; zwf753@foxmail.com; 15209809633@163.com; jinjielin1203@hnu.edu.cn).

Yicheng Zhou and Yosuke Nakanishi are with the Graduate School of Environment and Energy Engineering, Waseda University, Tokyo 169-8050, Japan (e-mail: zhou.yicheng@aoni.waseda.jp; zhouycjp2000@gmail.com).

Color versions of one or more figures in this article are available at <https://doi.org/10.1109/TSG.2022.3173964>.

Digital Object Identifier 10.1109/TSG.2022.3173964

the energy connections of MES are closer, and it realizes a balance between energy supply and consumption through the interaction of various energy in energy conversion and storage devices [2], [3]. What's more, it is necessary to accurately predict the short-term load of MES in advance ensuring economic dispatch and efficient operation. However, due to the interactive structure, the cooling, heating and electric loads of MES are different from the traditional electrical load in the single power system. Multiple loads not only fluctuate more randomly in different seasons, but also the connection among them is more complicated, which brings greater challenges to the load forecasting of MES.

In terms of the traditional independent energy system, load influencing factors mainly include historical load, the weather and date types. However, the mutual conversion of multiple energy sources leads to the coupling relationship of different loads in the MES. The current research has shown that the coupling relationship between cooling, heating, and electric loads is the important factor affecting the load forecasting for MES. Reference [4] adopts Pearson correlation analysis to quantitatively describe the coupling relationship among electric, cooling and heating loads. Spearman correlation analysis is carried out on cooling, heating and electric loads in [5], which shows that the coupling information among different loads can improve the effect of load forecasting. Reference [6] transmits the coupling information among the cooling, heating and electric loads to the forecasting model by the shared weight mechanism, which is based on the multi-task learning method. Reference [7] puts forward a synergistic electric load forecasting model based on the correlation analysis and the constructed load indexes, which shows that the coupling relationship among loads can improve the accuracy of load forecasting.

The above research works show that it is necessary for load forecasting to consider the coupling relationship among multiple loads. However, the current research still has some shortcomings. Firstly, loads of MES are greatly affected by the seasonal changes. The above-mentioned research only considers the coupling correlation among the loads throughout the year, and there is a lack of research work concerning on the changes of load coupling relationship in different seasons. Secondly, the above-mentioned load forecasting method has certain limitations. Multi-task learning may increase the shared

noise when the load fluctuates greatly [6], and the synergistic forecasting method [7] combines the prediction results of multiple indicators, which may cause the accumulation of forecasting errors. Thus, the load fluctuations in different seasons should be considered to improve the performance of load forecasting.

For short-term load forecasting, data-driven intelligent algorithms are effective techniques to solve load forecasting problems, compared with statistical methods such as linear regression and autoregressive integrated moving average. There are much literature reporting artificial intelligence algorithms for load forecasting combined with historical data [8]–[11]. As a kind of deep learning intelligent algorithm, Long Short-term Memory (LSTM) Neural Network can transmit effective temporal information [12], [13]. Many studies have confirmed that LSTM has strong non-linear mapping and self-learning ability, which achieves effective performance in short-term load forecasting. However, LSTM is a single-direction algorithm, and the global information of historical data will be ignored during the training process, which leads to a poor generalization of the prediction model [14]. Therefore, this paper chooses the BiLSTM in [15] for load forecasting, which can learn the regulation of loads in the time series more effectively by training the model in both positive and negative directions.

The aim of this paper is to investigate the coupling relationship between multiple loads in different seasons, and propose a combined load forecasting method for MES. The contribution of this paper can be summarized as follows:

- 1) Analyze the energy interaction mechanism and energy use structure of MES, deriving the energy balance matrix between multi-energy supply and multi-loads demand. The obtained interaction mechanism will help understand the energy flow law of MES and explain the reasons for the coupling relationship among different loads.

- 2) Investigate the energy consumption characteristics among multi-loads of MES under different seasons and time scales. The MIC correlation analysis method is used to calculate the correlation coefficients among the cooling, heating, and electric loads in each season, which facilitates analyzing the seasonal changes in the coupling relationship among multi-loads.

- 3) A combined load forecasting method of MES is proposed. Firstly, combined feature selection for each load in different seasons is carried out through the coupling relationship of multi-loads, and the corresponding input features of the load forecasting model are selected combinedly. Secondly, establish a combined forecasting model based on BiLSTM by sharing the hidden layer information of different load forecasting tasks, which take full use of the coupling information among multi-loads and effectively improve the accuracy of short-term load forecasting.

II. LOAD CHARACTERISTIC ANALYSIS OF MES

A. Energy Interaction Mechanism of MES

Fig. 1 shows the interaction structure of a typical MES. The structure is composed of three parts: the input, the middle, and the output layer. Firstly, the electric energy and

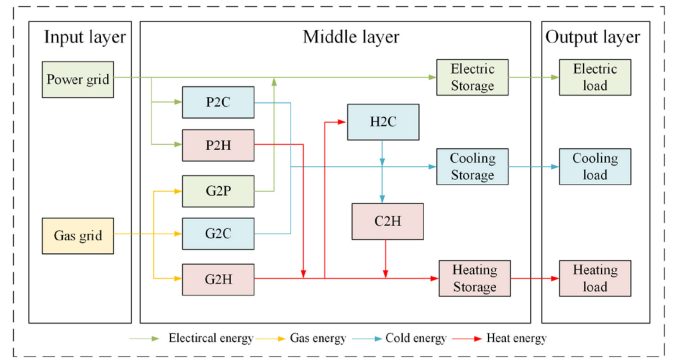


Fig. 1. The interaction structure of the multi-energy system.

natural gas provide energy source in the input layer. Then, the middle layer realizes energy conversion among cooling, heating, electric and gas by means of energy conversion devices such as Gas Turbine (GT), Compression Refrigerating Machine (CRM), Waste Heat Boiler (WHB) and so on. Among them, P2C represents the process of converting electricity into cooling, P2H represents the process of converting electricity into heating, and G2P represents the process of converting the gas into electricity similarly. In addition, different energy is stored through energy storage devices. The energy is transmitted to the output layer to meet the cooling, heating, and electric load demand of users.

It can be seen from Fig. 1 that the energy consumed by each load is not simply supported by one energy source, and the cooling, heating and electric energy will inevitably affect each other during energy conversion. Thus, the cooling, heating and electric loads are coupled, and it is necessary to consider the energy interaction mechanism in order to accurately predict the load demand of MES. This paper derives the energy balance matrix between multi-energy supply and multi-load demand, as shown in (1), which can help understand the energy interaction mechanism and the coupling relationship of multi-loads.

$$\begin{bmatrix} L_e \\ L_h \\ L_c \end{bmatrix} = \underbrace{\begin{bmatrix} \eta_{ee}\alpha_{ee} & \eta_{he}\alpha_{he} & \eta_{ce}\alpha_{ce} \\ \eta_{eh}\beta_{eh} & \eta_{hh}\beta_{hh} & \eta_{ch}\beta_{ch} \\ \eta_{ec}\beta_{ec} & \eta_{hc}\beta_{hc} & \eta_{cc}\beta_{cc} \end{bmatrix}}_{M1} \underbrace{\begin{bmatrix} P_{Ee} \\ P_{Eh} \\ P_{Ec} \end{bmatrix}}_{P_E} + \underbrace{\begin{bmatrix} \eta_{ee}\beta_{ee} & \eta_{he}\beta_{he} & \eta_{ce}\beta_{ce} \\ \eta_{eh}\beta_{eh} & \eta_{hh}\beta_{hh} & \eta_{ch}\beta_{ch} \\ \eta_{ec}\beta_{ec} & \eta_{hc}\beta_{hc} & \eta_{cc}\beta_{cc} \end{bmatrix}}_{M2} \underbrace{\begin{bmatrix} P_{Ge} \\ P_{Gh} \\ P_{Gc} \end{bmatrix}}_{P_G} - \underbrace{\begin{bmatrix} \eta_{ee}\gamma_{ee} & \eta_{he}\gamma_{he} & \eta_{ce}\gamma_{ce} \\ \eta_{eh}\gamma_{eh} & \eta_{hh}\gamma_{hh} & \eta_{ch}\gamma_{ch} \\ \eta_{ec}\gamma_{ec} & \eta_{hc}\gamma_{hc} & \eta_{cc}\gamma_{cc} \end{bmatrix}}_{M3} \underbrace{\begin{bmatrix} S_e \\ S_h \\ S_c \end{bmatrix}}_S \quad (1)$$

where P_E and P_G are the energy input vector, which represent electric and gas energy provided by energy suppliers; S is the intermediate vector, which represents the energy storage system that stores various forms of energy; L is the output vector, which represents the energy demand of users. Among them, e , h , c and g respectively represent electric, heating,

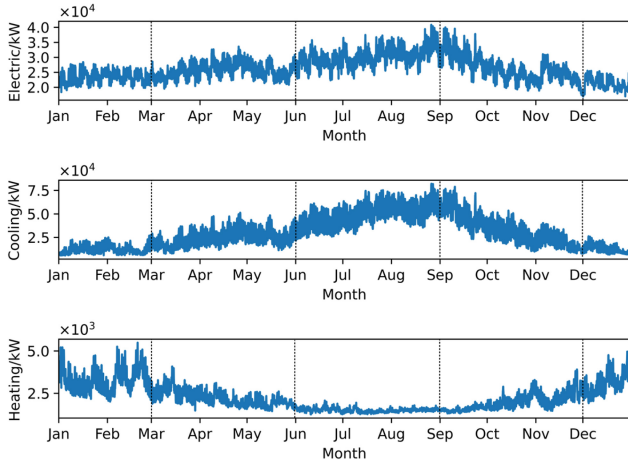


Fig. 2. Seasonal variation curve of multiple loads in one year.

cooling, and gas energy forms in the MES. M_1 and M_2 represent the coupling relationship matrix of energy conversion, while M_3 represents the coupling relationship matrix of energy storage; η represents the efficiency of energy conversion and storage; α , β and γ represent the distribution ratio of energy conversion and storage.

It can be seen from (1) that the initial energy sources of the cooling, heating and electric loads are from electric and gas. The energy conversion equipment consumes electric and gas to obtain the cooling, heating and electric energy, and stores the excess energy. In the process of using multiple energy sources, each energy source influences each other through the coupling conversion matrix of M_1 , M_2 , and M_3 , since the conversion efficiency of the conversion devices changes nonlinearly, the conversion process between different energy involves linear and nonlinear relationships. Therefore, during the interaction of MES, there will be a tighter coupling relationship between the cooling, heating, and electrical loads, which needs to be considered.

B. Load Characteristics Analysis in Different Seasons

The MES includes cooling, heating, and electric loads, and these loads are affected by factors such as climatic conditions, energy consumption habits, social development level, and date types. The multi-loads present different seasonal characteristics due to the different weather conditions. In this paper, the user-level MES data of the Arizona State University Tempe campus are taken as an example. The seasonal characteristics of cooling, heating and electric loads are focused on.

The seasons are divided as follows: spring is from March to May, summer is from June to August, autumn is from September to November, and winter is from December to February. Fig. 2 shows the curve of multi-loads fluctuation in 2019. It can be seen that the electric and cooling load curves have similar trends; both of them are characterized by an increase in summer and a decrease in winter, however, the heating load has the opposite characteristic. This shows that electric, cooling and heating loads are highly complementary in summer and winter. Judging from the trend of quarterly changes in Fig. 2, the changes in the cooling, heating, and

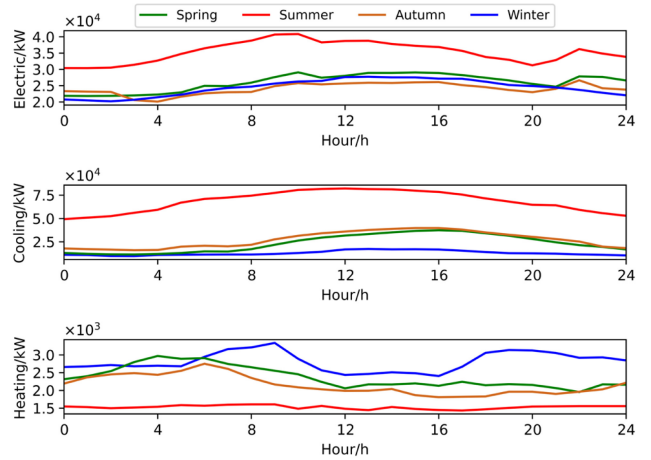


Fig. 3. Typical daily load curve of multi-energy systems in different seasons.

electric loads are smooth in spring. As the temperature rises in summer, the electric and cooling loads gradually increase until reaching a peak in September, while the demand of heating load drops to the lowest level with tiny change. In autumn, the electric and cooling loads show a downward trend when the temperature gradually decreases, while the heating load has gradually shown an upward trend. In winter, the electric load changes steadily, the cooling load drops to a lower level, and the heating load rises to reach the annual peak.

Fig. 3 shows the typical daily 24-hour fluctuation curve of cooling, heating and electric loads for each season. The value of the electric load is the largest in summer. There will be two peaks in the daily curve, appearing around 10:00 and 22:00, which are related to the daily living habits of residents. While the change of electric load in winter is relatively flat and the peak phenomenon is not apparent. The cooling load also has the largest value in summer, reaching its peak at 12:00, and the peaks of the other seasons are delayed at 16:00. The daily curve of cooling load is similar in spring and autumn, and the demand for cooling load in winter is the lowest. The heating load maintains the highest value in winter and there are two peaks, appearing at 9:00 and 20:00, respectively. In addition, the value of heating load in spring is slightly higher than that in autumn and the peak-valley difference in autumn is smaller. The daily curve of heating load is a single peak in spring and autumn, with the peak in spring at about 4:00 and in autumn at about 6:00.

However, the heating demand is a rigid demand in summer, so the daily curve of heating load is the smallest and hardly fluctuates.

It can be seen from the above analysis that the load characteristics in different seasons are quite different, and the trends of the cooling, heating and electric loads are similar or complementary in the four seasons. Therefore, analyzing the loads according to season can more precisely grasp the fluctuation law of multi-loads.

C. Loads Correlation Analysis in Different Seasons

Since MES provides energy to loads by means of energy conversion and storage devices, there is a coupling relationship

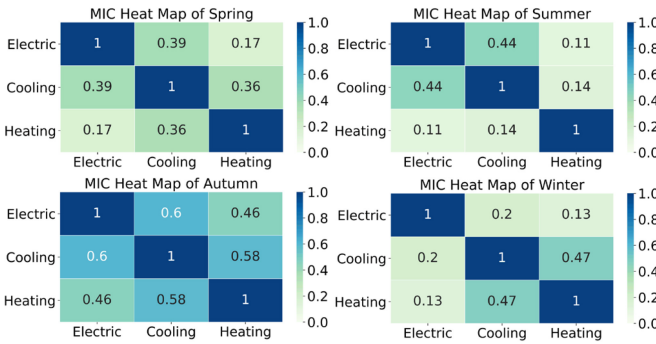


Fig. 4. MIC heat map of loads in different seasons.

between cooling, heating and electric loads. The load changes in different seasons also show similar or complementary phenomena, so the change of one load will correspondingly transfer information to other loads, and different loads affect each other in different seasons. It is important to analyze load-related influencing factors for load forecasting. In order to measure the correlation between different loads, the MIC method [16]–[18] is used to analyze the linear and non-linear correlation degree of the multiple loads.

The calculation of MIC is based on the principle of mutual information, which measures the correlation between two variables through joint probability [19]. Compared with the linear correlation analysis of Pearson in [20], MIC obtains the linear or nonlinear correlation based on the mutual information calculation of the sample grid division, so it can measure the complex correlation among multiple loads and lay the foundation for more accurate feature selection for load forecasting. From the analysis of equation 1, it can be seen that the loads of MES include not only the addition and subtraction linear relationship of electric energy, gas energy and energy storage, but also the complex linear and nonlinear relationship of the energy conversion and energy storage matrix M. Therefore, in order to analyze the coupling correlation between loads more accurately, the MIC algorithm is adopted, which has the advantages of being able to measure linear and nonlinear correlations at the same time, with low computational complexity and excellent robustness. The calculation equation of MIC is as follows:

$$MIC(x, y) = \max_{a*b < S} \left(\frac{\int \int p(x, y) \log_2 \frac{p(x, y)}{p(x)p(y)}}{\log_2 \min(a, b)} \right) \quad (2)$$

where a and b represent the number of grids divided in the x -axis and y -axis directions; S is the total number of grids, which is the 0.6th power of the data samples; $P(x, y)$ represents the probability that the variable samples are distributed in the grid x and y . The mutual information is calculated by the joint probability of the sample distribution in the grid, and the MIC takes the maximum value of the normalized mutual information.

Fig. 4 shows the MIC heat map of the loads in different seasons, revealing the seasonal correlation among loads of MES: 1) There is a linear or non-linear correlation between cooling load and heating load. In MES, the correlation between electric load and cooling load is stronger than that between

TABLE I
COMBINED SELECTION FOR INPUT FEATURE OF MULTIPLE LOADS

| The Number of MIC Greater Than Threshold | Combined Selection of Input Feature Method |
|--|--|
| 0 | Select each load individually |
| 1 | Choose two loads with MIC values greater than threshold as combined feature, and the other load alone as a feature |
| 2 | Select the cooling, heating and electric loads together as features |
| 3 | Select the cooling, heating and electric loads together as features |

electric load and heating load; 2) The MIC correlation among the cooling, heating, and electrical loads changes in different seasons.

It can be seen from Fig. 4 that the MIC correlation coefficient between electric and cooling load in Spring is greater than 0.3, indicating that the connection between electric and cooling is close. Similarly, the relationship between cooling and heating load is also the same. However, the MIC of electric and heating load is only 0.17, which shows the correlation is weak. In Summer, the correlation between cooling and electric loads reaches 0.44, indicating the correlation is strong, which meets the law that a large number of electric refrigeration equipment are used in summer. In autumn, the MIC between loads are all above 0.45, showing the cooling, heating and electric loads influence each other and the correlation among them is strong. In winter, the MIC of heating load and cooling load is 0.47, so they have a strong correlation.

This paper focuses on the coupling relationship between multiple loads in different seasons and realizes the sharing of information between loads by the combined load forecasting method, thereby improving the accuracy of load forecasting.

III. COMBINED LOAD FORECASTING METHOD

A. Combined Selection of Input Feature

The key to load forecasting is to select the features most relevant to the load as the input of the forecasting model. According to the coupling relationship between loads, this paper proposes a combined method to select input features. Firstly, calculate the correlation between the electric, cooling and heating load in each season. Then, count the number of MIC correlation coefficients in each season whose value is greater than the threshold, and select the input features by the statistical results of MIC. In term of the MIC analysis results in different seasons, different input features are selected to construct the corresponding load forecasting model. The specific feature selection is shown in Table I, and the combined input feature is obtained in the following scenarios:

Scenario 1: Electric, cooling and heating load are combined selected as input features. The number of MIC values greater than the threshold is 2 or 3, and the input features are determined by the three types of loads.

Scenario 2: Two types of loads are selected as input features together. The number of loads with a MIC value greater than the threshold is 1. Two types of loads with MIC values greater than threshold are selected together as input features, while the

other type of load only selects its own historical data as input features.

Scenario 3: Electric, cooling and heating loads are separately used as input features. The number of MIC values greater than the threshold is 0, and the input feature is every single type of load.

B. BiLSTM Model

BiLSTM is a neural network that contains a forward LSTM layer and a backward LSTM layer [21]. The basic structural unit and algorithm of BiLSTM are derived from LSTM. Taking the LSTM at time t as an instance, the LSTM unit will input the last output result $y^{(t-1)}$ and the current variable $x^{(t)}$. Firstly, it is necessary to determine the forgetting content of the cell state $c^{(t-1)}$, so the input variables are calculated through the forgetting gate to obtain the forgetting factor $f^{(t)}$. Next, the input variables $x^{(t)}$ and $y^{(t-1)}$ determine which new information of the cell state needs to be updated through the sigmoid activation function of the input gate, and a new cell candidate state $u^{(t)}$ is created through the tanh activation function of the input gate.

The key function of the input gate and the forgetting gate is to control information preservation and to forget, thus a new neuron cell state $c^{(t)}$ is established to update the neuron cell state. Finally, the output gate $o^{(t)}$ uses the sigmoid activation function to determine part of the output information, which is multiplied by the new cell state $c^{(t)}$ after the tanh transformation to obtain the output result $y^{(t)}$. The calculation equations of LSTM are as follows:

$$f^{(t)} = \sigma(W_{fy}y^{(t-1)} + W_{fx}x^{(t)} + b_f) \quad (3)$$

$$i^{(t)} = \sigma(W_{iy}y^{(t-1)} + W_{ix}x^{(t)} + b_i) \quad (4)$$

$$u^{(t)} = \tanh(W_{uy}y^{(t-1)} + W_{ux}x^{(t)} + b_u) \quad (5)$$

$$c^{(t)} = i^{(t)} \cdot u^{(t)} + f_t \cdot c^{(t-1)} \quad (6)$$

$$o^{(t)} = \sigma(W_{oy}y^{(t-1)} + W_{ox}x^{(t)} + b_o) \quad (7)$$

$$y^{(t)} = o^{(t)} \cdot \tanh(c^{(t)}) \quad (8)$$

where W_{fy} , W_{fx} , W_{ix} , W_{iy} , W_{uy} , W_{ox} , W_{oy} are weight matrices for the corresponding gates of the network, while the b_f , b_i , b_u , b_o are the bias matrices; σ and \tanh represent the sigmoid and tanh activation function respectively.

Considering the forward and backward information of time series data can effectively improve forecasting accuracy. Compared with the unidirectional state transmission in the standard LSTM, the structure of BiLSTM can learn the regulation in the forward and backward directions simultaneously. By the bidirectional time series feature extraction, BiLSTM has more superior performance to LSTM, and its network structure is shown in Fig. 5. By the combination of two-direction LSTM, the output result of BiLSTM is calculated as the following:

$$y'^{(t)} = g(W_{y'f}y_f^{(t)} + W_{y'b}y_b^{(t)} + b_y) \quad (9)$$

where y_f and y_b represent the output result of forward LSTM and backward LSTM. $W_{y'f}$ and $W_{y'b}$ are the weight matrices

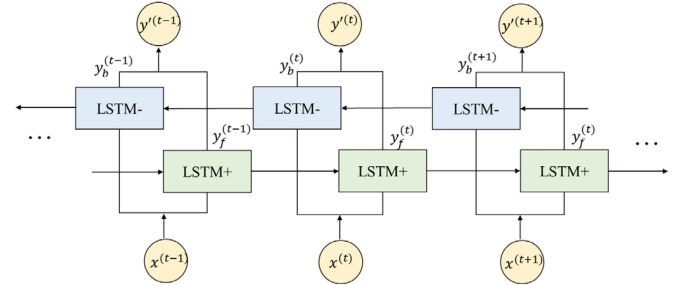


Fig. 5. The network structure of BiLSTM.

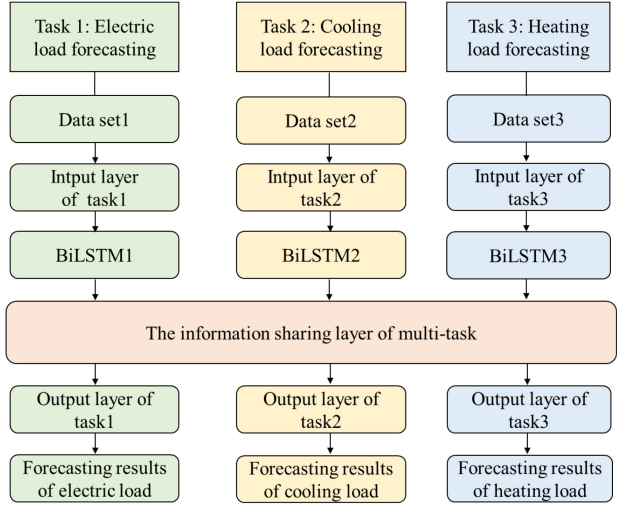


Fig. 6. The combined load forecasting framework based on multi-task learning.

of the calculated output result $y'^{(t)}$, while the b_y is the output bias matrices; g represents the output layer activation function.

C. Multi-Task Learning Based Combined Loads Forecasting

The proposed load forecasting of MES lies in the coupling relationship and mutual influence between loads and selects multiple related loads as the input for forecasting. In terms of model training, it can also be combined with multiple types of load forecasting tasks, that is, the multi-task learning [22], which shares relevant information between multiple load forecasting tasks to improve the accuracy of forecasting. It can be seen from Fig. 1 that there is a coupling relationship in the conversion of cooling, heating and electrical loads, and the correlation between cooling, heating and electrical loads needs to be further explored. Therefore, through this multi-task learning method, the information between the cooling, heating and electric loads can be shared, so that the information on the internal conversion of the cooling, heating, and electric loads can be excavated. The combined load forecasting framework based on multi-task learning is shown in Fig. 6.

The combined load forecasting method includes three tasks of cooling, heating and electric load forecasting. Firstly, input the data set obtained by the feature combination selection, and establish the corresponding BiLSTM for learning. Then, the three tasks will train together by the information sharing layer of multi-task learning, which effectively merges the coupling

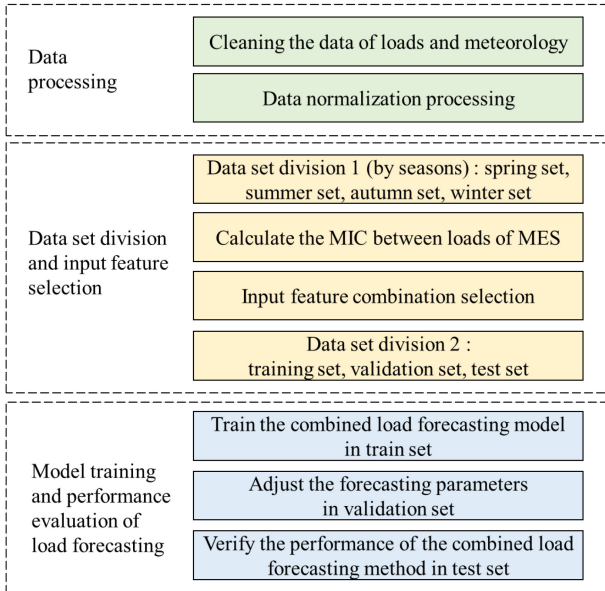


Fig. 7. The process of combined load forecasting.

information between the cooling, heating, and electric load forecasting tasks. The loss function of multi-task learning is optimized by a dynamic weighting method shown in (10), the weights are dynamically adjusted according to the learning stages of forecasting tasks [23].

$$L = \sum_{n=1}^N w_n(t) L_n \quad (10)$$

where N is the number of training tasks, w_n and L_n represent the weights matrices and loss function of the n -th task respectively.

D. Modeling Process

Based on the above analysis, the combined load forecasting process is shown in Fig. 7. The steps of short-term combined load forecasting based on the coupling relationship of loads and BiLSTM multi-task learning are as follows:

(1) Data preprocessing. Firstly, eliminate the outliers in the load and meteorological data, and fill in the missing values by the data cleaning method. Then, convert data dimensions into the range of 0-1 by data normalization.

(2) Data set division and input feature selection. Divide the data set into different seasons, then calculate the MIC between the loads, and realize combined feature selection according to the correlation of the loads in each season. Finally, divide the data of each season into the training, validation and test set.

(3) Model training and performance evaluation of load forecasting. Firstly, input the training set to train the forecasting model. Then, the performance of the training model on the validation set is evaluated, and the optimal parameters of the model are obtained by grid search [24]. Finally, verify the load forecasting performance on test set by setting up the comparative experiments.

In order to compare the load forecasting performance, Root Mean Squared Error (RMSE) in [25] and Mean Absolute

Percentage Error (MAPE) in [26] are used as the evaluation index to measure the deviation between the forecasting value and the actual value.

$$MAPE = \frac{1}{n} \sum_{i=1}^n \frac{|y'_i - y_i|}{y_i} \times 100\% \quad (11)$$

$$RMSE = \sqrt{\frac{1}{n} \sum_{i=1}^n (y'_i - y_i)^2} \quad (12)$$

where n is the number of samples, y_i and y'_i represent the actual value and the forecasting value of the load, respectively.

IV. CASE STUDIES

In this paper, the historical data of the Tempe campus at Arizona State University are selected for research [27]. Mainly for the energy data in the Tempe campus, it is a user-level MSE. Moreover, the meteorological data comes from the official website of the National Renewable Energy Laboratory [28], which includes the meteorological data of the Tempe campus. It contains 1461 days' hourly load and meteorological data from 2016 to 2019. Considering the impact of the data in the same period last year, the load forecasting is based on the load from 2017 to 2019, with one hour as the forecast step. Before data processing, the cooling and heating load data are converted with kW as the base unit. The unit conversion rules of the cooling and heating load are as follows: 1 kW = 0.284 Tons and 1 kW = 0.0034 mmBtu. All experiments are based on the PyCharm platform, using the Python language to implement the load forecasting algorithm under the Keras deep learning library.

A. Data Processing

In general, the raw data will have some outliers and missing values due to the problems such as the transmission interference of the data devices, which affect the accuracy of the forecasting model and may lead to poor forecasting results. Therefore, it is necessary to obtain complete and high-quality data through data cleaning. In this paper, the quartile method is used to eliminate the outliers, which converts the outliers into missing data, and linear interpolation is used to fill the missing data.

When multiple input variables are used for load forecasting, the dimensions and magnitudes of different variables are quite different. In order to consider the role of each variable equally, it is necessary to normalize the variables. According to the following normalization equation, the data values are all reduced to between 0 and 1:

$$x' = \frac{x - (x_{\max} + x_{\min})}{(x_{\max} - x_{\min})} \quad (13)$$

where x' and x represent the variable values before and after normalization, x_{\min} and x_{\max} respectively represent the minimum and the maximum values in the sample variables.

B. Data Set Division and Input Feature Selection

According to the month of the season, the data from 2017 to 2019 are divided into four parts. Table II shows the number of

TABLE II
THE DAYS OF DATA SET IN EACH SEASON

| | Spring | Summer | Autumn | Winter |
|----------------------|--------|--------|--------|--------|
| The days of data set | 276 | 276 | 273 | 270 |

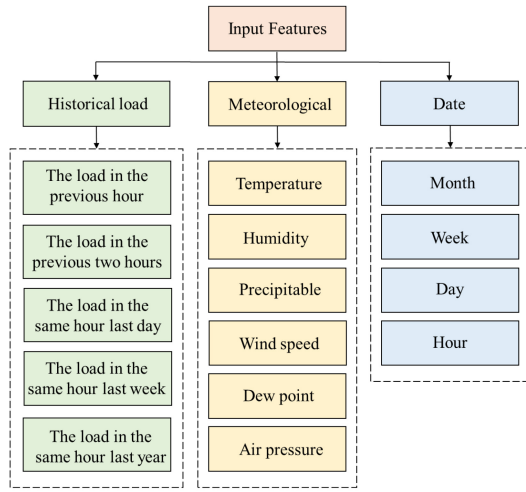


Fig. 8. Input features of load forecasting model.

days included in different seasons. Each season, the division ratio of the training set, validation set, and test set is 8:1:1.

The input features are one of the most important factors that affect the results of load forecasting, so it is necessary to select the input features which have a strong correlation with the load in order to predict the future changes of the multiple loads more accurately. Generally, the factors that affect load mainly include historical load, the meteorological and date information. Based on the existing data, this paper considers that the load change has a strong correlation with the recent and last year's historical data, so the input feature selection contains the historical load data. In addition, there is a strong correlation between load and meteorological data. Especially for the cooling and heating load of a multi-energy system, there are different requirements under different temperature conditions. Therefore, temperature, humidity, precipitable, wind speed, dew point, and air pressure are selected as input features. Besides, the load demand is different during holidays, weekdays and weekends. Therefore, adding month, day of week, day of the date and hour to the forecast model as input features, the selected input features are shown in Fig. 8.

According to the feature combination selection method in Section III, the MIC correlation coefficient between loads of each season from 2017 to 2019 is calculated, as shown in Table III. The feature selection results between loads are shown in Table IV. In order to ensure that the number of feature selection is simplified and the prediction effect is good, the threshold of feature selection in this paper is 0.3. In Spring, the MIC correlation coefficients of electrical load and cooling load, cooling load and heating load are 0.408 and 0.425, respectively. The number of MIC greater than 0.3 is 2, so the historical data of the cooling, heating and electrical loads are combined as the input features. In summer, the MIC between

TABLE III
THE MIC CORRELATION COEFFICIENT OF MULTIPLE LOADS

| Seasons | Electric with Cooling | Electric with Heating | Cooling with Heating |
|---------|-----------------------|-----------------------|----------------------|
| Spring | 0.408 | 0.207 | 0.425 |
| Summer | 0.351 | 0.112 | 0.098 |
| Autumn | 0.562 | 0.445 | 0.588 |
| Winter | 0.221 | 0.110 | 0.443 |

TABLE IV
RESULTS OF FEATURE SELECTION BETWEEN LOADS

| Seasons | Forecasting Model | Combined Selection of Input Feature |
|---------|-------------------|-------------------------------------|
| Spring | Electric load | Electric, cooling and heating loads |
| | Cooling load | Electric, cooling and heating loads |
| | Heating load | Electric, cooling and heating loads |
| Summer | Electric load | Electric and cooling loads |
| | Cooling load | Electric and cooling loads |
| | Heating load | Heating load |
| Autumn | Electric load | Electric, cooling and heating loads |
| | Cooling load | Electric, cooling and heating loads |
| | Heating load | Electric, cooling and heating loads |
| Winter | Electric load | Electric load |
| | Cooling load | Cooling and heating loads |
| | Heating load | Cooling and heating loads |

electric load and cooling load is 0.351, indicating that the coupling relationship between electric load and cooling load is strong. Therefore, the electric load and cooling load are selected as the input features of the electric load forecasting model and the cooling load forecasting model, while the heating load forecasting model only selects historical heating load as the input load feature for individual prediction. In autumn, the MIC of the three loads is all greater than 0.3, indicating that the three types of loads have a strong correlation, so they are all selected as input features. In the same way, the cooling load and the heating load have larger MIC in winter, so the cooling load and the heating load are selected as input for the forecasting of cooling and heating load, while the electric load is individually selected as the input feature of the electric load forecasting model.

C. Performance of Combined Load Forecasting Considering the Input Feature Selection and BiLSTM

In order to explore the impact of the coupling relationship between loads on load forecasting, verify the effectiveness of the combined selection of input features and test the performance of the BiLSTM algorithm proposed in this paper, four cases are set up in this section. The specific input variables and forecasting models of each case are as the following:

Case 1: The electric, cooling and heating loads are forecasted separately, without considering the correlation

TABLE V
PARAMETER RANGE OF FORECASTING MODEL

| Parameter Type | Number of Hidden Neurons | Learning Rate | Batch Size |
|----------------|--------------------------|----------------|------------|
| Scope | [32, 64, 128, 256] | [0.01, 0.1, 1] | [24, 168] |

relationship among loads, and the LSTM is used to establish the load forecasting model.

Case 2: The electric, cooling and heating loads are forecasted combinedly, considering the correlation relationship among loads by proposed feature combination selection in Table III, and the LSTM is used to establish the load forecasting model.

Case 3: The electric, cooling and heating loads are forecasted separately, without considering the correlation relationship among loads, and the BiLSTM is used to establish the load forecasting model.

Case 4: The electric, cooling and heating loads are forecasted combinedly, considering the correlation relationship among loads by proposed feature combination selection in Table III, and the BiLSTM is used to establish the load forecasting model.

In the cases, a single hidden layer of LSTM and BiLSTM is set, in which the activation function is ReLU and the loss function is mean square error. In order to prevent the model from overfitting, a dropout with 0.2 is added after the LSTM and BiLSTM layer and L2 regularization with the regular parameter of 0.01 is set. The hidden layer of the network is 1. The rest of parameters are determined by the grid search method. The specific tuning process of the grid search method is as follows: First, input validation set into the training model. The model has not been trained on validation set, which can ensure the fairness and effectiveness of the tuning process. Then, perform loop traversal within the parameter range of Table V. Finally, get the forecasting result of 3-fold cross-validation [29]. The parameters that perform best in validation set are retained as the final parameters of the forecasting model.

Through the learning of the model, the load forecasting results are obtained as follows: Fig. 9 to Fig. 12 show the cooling, heating, and electric load forecasting results for one week of each case in the different seasons. Tables VI to IX show the forecasting error of each case in the test set.

From the aspect of feature selection based on the relationship of load coupling, the accuracy of the forecasting results with related loads combinations as the input features is higher. The average RMSE and MAPE of case 2 are 88.52 kW and 0.4% smaller than case 1, respectively. The average RMSE and MAPE of case 4 are 111.82 kW and 0.5% smaller than case 3, respectively. Especially in the autumn load forecasting, the forecast accuracy using multiple related loads as input is greatly improved, which shows that loads of MES have a coupling relationship and influence each other. To sum up, the forecasting model can learn more effective information through multiple loads as input, which verifies the superiority of the combined feature selection in load forecasting.

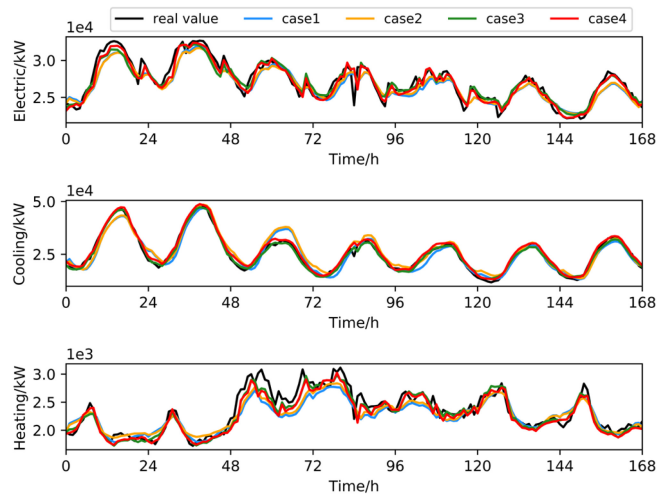


Fig. 9. Forecasting results of cooling, heating and electric loads in spring.

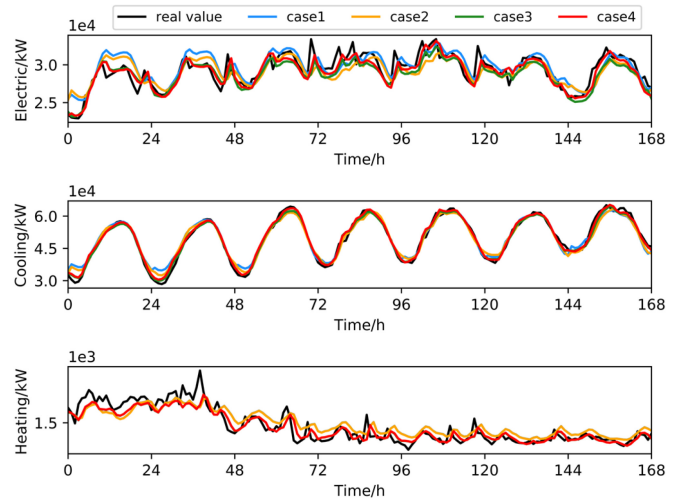


Fig. 10. Forecasting results of cooling, heating and electric loads in summer.

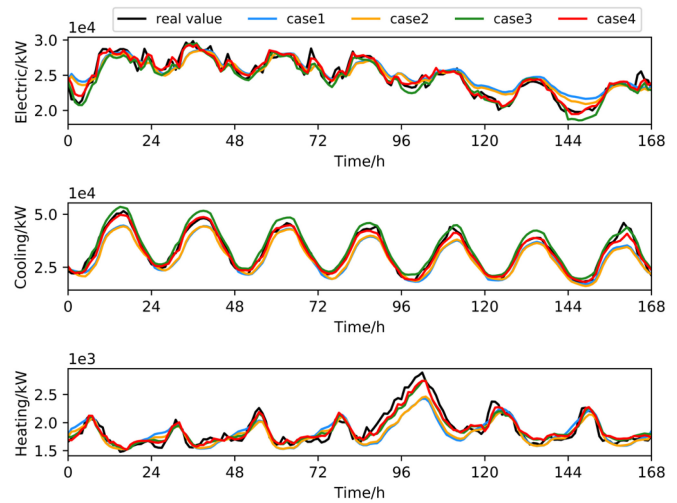


Fig. 11. Forecasting results of cooling, heating and electric loads in autumn.

In order to reflect the advantages of the BiLSTM forecasting model, a comparison of the BiLSTM and LSTM load forecast performance is carried out. The forecasting errors of

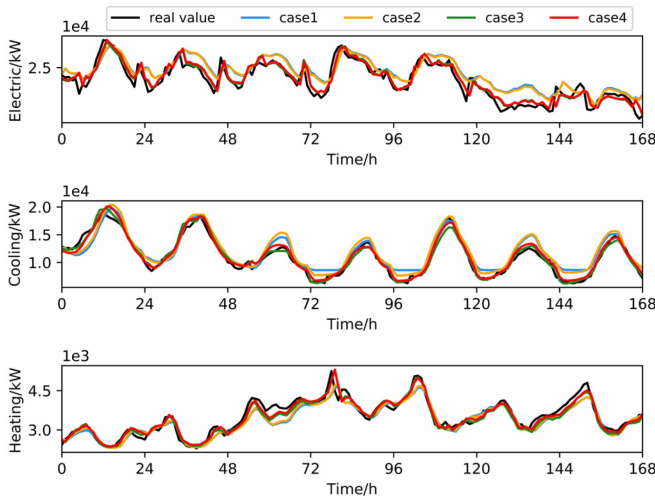


Fig. 12. Forecasting results of cooling, heating and electric loads in winter.

TABLE VI
LOAD FORECASTING RESULTS OF MULTI-ENERGY SYSTEM IN SPRING

| Load Type | Method | RMSE(kW) | MAPE(%) |
|---------------|--------|----------|---------|
| Electric load | Case1 | 1096.770 | 3.326 |
| | Case2 | 1043.082 | 3.155 |
| | Case3 | 858.368 | 2.596 |
| | Case4 | 820.380 | 2.342 |
| Cooling load | Case1 | 2546.694 | 7.892 |
| | Case2 | 2416.311 | 7.877 |
| | Case3 | 1590.235 | 4.974 |
| | Case4 | 1262.273 | 3.793 |
| Heating load | Case1 | 144.038 | 5.826 |
| | Case2 | 137.840 | 5.625 |
| | Case3 | 106.345 | 4.054 |
| | Case4 | 103.015 | 3.909 |

TABLE VII
LOAD FORECASTING RESULTS OF MULTI-ENERGY SYSTEM IN SUMMER

| Load Type | Method | RMSE(kW) | MAPE(%) |
|---------------|--------|----------|---------|
| Electric load | Case1 | 1580.595 | 4.092 |
| | Case2 | 1532.935 | 3.765 |
| | Case3 | 1489.584 | 3.654 |
| | Case4 | 1147.105 | 2.662 |
| Cooling load | Case1 | 3306.754 | 4.894 |
| | Case2 | 2853.829 | 4.315 |
| | Case3 | 1662.756 | 2.383 |
| | Case4 | 1634.732 | 2.273 |
| Heating load | Case1 | 55.580 | 2.951 |
| | Case2 | 55.153 | 2.913 |
| | Case3 | 51.567 | 2.428 |
| | Case4 | 50.982 | 2.393 |

case 3 and case 4 in each season are significantly smaller than case 1 and case 2. Besides, it can be seen from the figures that the load forecasting curve of BiLSTM fits the real load curve

TABLE VIII
LOAD FORECASTING RESULTS OF MULTI-ENERGY SYSTEM IN AUTUMN

| Load Type | Method | RMSE(kW) | MAPE(%) |
|---------------|--------|----------|---------|
| Electric load | Case1 | 1654.918 | 5.396 |
| | Case2 | 1533.195 | 4.848 |
| | Case3 | 1085.092 | 3.672 |
| | Case4 | 784.795 | 2.505 |
| Cooling load | Case1 | 3426.052 | 11.884 |
| | Case2 | 3154.371 | 10.771 |
| | Case3 | 2029.551 | 7.686 |
| | Case4 | 1864.566 | 7.560 |
| Heating load | Case1 | 173.617 | 6.278 |
| | Case2 | 160.415 | 5.441 |
| | Case3 | 134.068 | 5.145 |
| | Case4 | 111.804 | 4.280 |

TABLE IX
LOAD FORECASTING RESULTS OF MULTI-ENERGY SYSTEM IN WINTER

| Load Type | Method | RMSE(kW) | MAPE(%) |
|---------------|--------|----------|---------|
| Electric load | Case1 | 1056.928 | 4.001 |
| | Case2 | 1052.522 | 3.919 |
| | Case3 | 773.284 | 2.802 |
| | Case4 | 767.517 | 2.728 |
| Cooling load | Case1 | 1505.984 | 10.317 |
| | Case2 | 1363.717 | 9.068 |
| | Case3 | 977.118 | 6.814 |
| | Case4 | 880.775 | 5.324 |
| Heating load | Case1 | 224.608 | 5.203 |
| | Case2 | 213.604 | 5.068 |
| | Case3 | 160.966 | 3.865 |
| | Case4 | 149.004 | 3.521 |

better, which indicates that BiLSTM can learn the fluctuation regulation of the time series more effectively, thereby greatly improving the accuracy of cooling, heating and electric load forecasting of multi-energy system.

Moreover, from the forecast results of the different seasons, the fluctuations of loads in spring, summer and winter are more regular, and the forecasting performance is better. The forecasting results of the multiple loads in summer have the smallest error, while the cooling load fluctuates greatly in autumn and winter, which causes the MAPE increases a little between 5% and 7%. From the forecasting of the cooling, heating and electricity load, the forecasting error of the electric load and the heating load is small, and the change is relatively stable within 5%, which indicates the effectiveness of the proposed forecasting method based on feature selection and BiLSTM, with smaller errors and higher forecasting accuracy.

Furthermore, it can be obtained that case 4 has the best performance by adopting feature combination selection and BiLSTM. For case 4, comparing the load forecasting results of

TABLE X
PARAMETER RANGE OF SVM

| Parameter Type | Kernel Function | Kernel Function Coefficient | Penalty Coefficient |
|----------------|-----------------|-----------------------------|-------------------------|
| Scope | [Linear, RBF] | [0.01, 0.1, 1, 10, 100] | [0.01, 0.1, 1, 10, 100] |

TABLE XI
PARAMETER RANGE OF RF

| Parameter Type | Number of Trees | Maximum Depth |
|----------------|---|---------------|
| Scope | [50, 100, 150, 200, 250, 300, 350, 400] | [10, 50, 100] |

the four seasons, it can be found that the electric load forecasting effect is the most stable, and the MAPE of the four seasons is all within 3%. The cooling load forecasting effect is best in summer, and the MAPE is 2.273%. The autumn forecasting effect is poor, and the MAPE is 7.560%. It is mainly due to the obvious characteristics of summer cooling load. Choosing the cooling and electric load combination forecasting can better mine the characteristics of cooling load. While the cooling load fluctuates greatly in autumn, and the heating and electric loads affect each other. The characteristics of cooling load are not as obvious in autumn, so the forecasting performance has declined. The heating load forecast performance is better in summer and winter, where the MAPE is 2.393% and 3.521%, respectively. The reason is that the heating load in summer is a rigid load with small fluctuations and is not strongly correlated with the cooling load and electric load. Therefore, individual forecasting can dig out the own law of heating load. The characteristics of heating load in winter are more obvious, and the combination selection of input features for forecasting can better dig out the law of heating load.

D. Performance of the Combined Load Forecasting Based on the Multi-Task Learning

In order to verify the effectiveness of the multi-task learning for the combined load forecasting method proposed in this paper, the MES load forecasting results of single-task learning and multi-task learning are compared on the basis of combined feature selection and BiLSTM. Among them, single-task learning is set as case 4 in Section III. For multi-task learning, a fully connected neural network is added after the BiLSTM layer as the multi-task learning shared layer. The number of neurons in the shared layer is 10.

In addition, common regression algorithms support vector machines (SVM), Random Forest (RF), and LSTM are also used to compare the load forecasting effects. The grid search is used to adjust the parameters of LSTM and BiLSTM and multi-task learning, and the parameter adjustment range refers to Table I. The parameter adjustment range of SVM and RF is shown in Table X and Table XI.

The cooling, heating and electric load forecasting results for one week are shown in Fig. 13, and the load forecasting errors in the different seasons are obtained in Table XII. The load forecasting curve of multi-task learning has a better fitting performance than single-task learning, and the curve is closer to the real load curve. Compared with the load forecasting

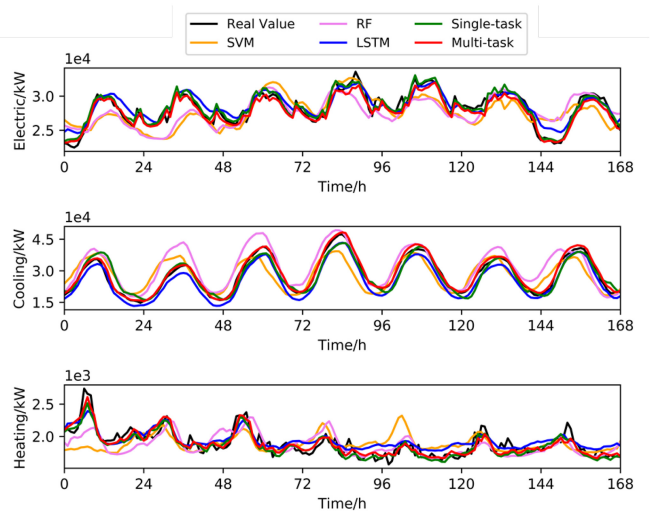


Fig. 13. The results of load forecasting.

TABLE XII
THE ERRORS OF LOAD FORECASTING

| Load Type | Method | MAPE(%) | | | |
|---------------|-------------|---------|--------|--------|--------|
| | | Spring | Summer | Autumn | Winter |
| Electric load | SVM | 6.334 | 7.188 | 6.867 | 6.432 |
| | RF | 5.987 | 6.309 | 5.466 | 5.965 |
| | LSTM | 3.155 | 3.765 | 4.848 | 3.919 |
| | Single-task | 2.342 | 2.662 | 2.505 | 2.728 |
| | Multi-task | 2.128 | 2.451 | 2.269 | 2.566 |
| Cooling load | SVM | 12.822 | 12.394 | 17.932 | 16.447 |
| | RF | 8.432 | 7.260 | 12.309 | 12.020 |
| | LSTM | 7.877 | 4.315 | 10.771 | 9.068 |
| | Single-task | 3.793 | 2.273 | 7.560 | 5.324 |
| | Multi-task | 3.579 | 2.265 | 7.453 | 5.154 |
| Heating load | SVM | 12.231 | 9.673 | 10.802 | 10.533 |
| | RF | 8.307 | 5.198 | 7.434 | 7.651 |
| | LSTM | 5.625 | 2.913 | 5.441 | 5.068 |
| | Single-task | 3.909 | 2.393 | 4.280 | 3.521 |
| | Multi-task | 3.724 | 2.188 | 4.105 | 3.213 |

based on single-task, the average MAPE of multi-task forecasting decreases from 3.6% to 3.4%. Compared with commonly used load forecasting algorithms, the MAPE of multi-task learning is the smallest and has the smallest change in the four seasons, indicating that the forecasting model has better robustness. Therefore, the multi-task learning can effectively use the shared information, which helps deep learning algorithms train better and improve the accuracy of respective load forecasting tasks.

From Table XII, in the horizontal direction, it can be seen that the electrical load forecasting performance of the four seasons is relatively stable. The forecasting performance of cooling load is the best in summer, and the forecasting of heating load in summer and autumn is better. It shows that

TABLE XIII
THE TRAINING TIME OF SINGLE-TASK AND MULTI-TASK

| Method | Training time(s) |
|-------------|------------------|
| Single-task | 10944 |
| Multi-task | 3732 |

the feature combination selection also reflects the degree of seasonal correlation between loads, and the forecasting accuracy characteristics of MES loads under seasonal changes. In the longitudinal direction, the prediction performance of different models is compared, and the multi-task learning accuracy is the highest, which shows that the multi-task learning model based on BiLSTM proposed is effective in improving the accuracy of load forecasting.

The training time of the model is also an important indicator to measure the computational efficiency of the model. It can be seen from Table XIII that it takes 10944 seconds to train single-task learning models and only 3732 seconds to train a multi-task learning model. Obviously, the combined load forecasting model based on multi-task has the advantages of smaller forecasting error and faster calculation speed, and it is suitable for the engineering application when requiring high forecasting accuracy and fast calculation speed.

V. CONCLUSION

This paper proposes a combined cooling, heating and electric load forecasting method based on BiLSTM multi-task learning, which is mainly improved on the feature selection and the forecasting models. The coupling relationship of cooling, heating and electric load in different seasons is investigated, including the combined selection of input feature and the multi-task learning model based on BiLSTM. This method can transmit information about the coupling relationship between loads via the fusion of features and models, which learns the regulation of cooling, heating, and electric loads better. The effectiveness of the combined forecasting method is verified by load forecasting cases in different seasons. The test results show that the proposed method significantly improves both load forecasting accuracy and the time cost of model training, which has a critical engineering application value in the MES.

REFERENCES

- [1] J. Zhu, H. Dong, and S. Li, "Review of data-driven load forecasting for integrated energy system," *Proc. CSEE*, vol. 41, no. 23, pp. 7905–7924, Dec. 2021.
- [2] N. Liu, J. Wang, and L. Wang, "Hybrid energy sharing for multiple microgrids in an integrated heat–electricity energy system," *IEEE Trans. Sustain. Energy*, vol. 10, no. 3, pp. 1139–1151, Jul. 2019.
- [3] W. Wu, J. Wu, and Z. Lei, "Park energy demand forecasting based on CSO optimized deep belief network," *Power Syst. Technol.*, vol. 45, no. 10, pp. 3859–3868, Oct. 2021.
- [4] Y. Yan and Z. Zhang, "Cooling, heating and electrical load forecasting method for integrated energy system based on SVR model," in *Proc. 6th Asia Conf. Power Elect. Eng. (ACPEE)*, Chongqing, China, 2021, pp. 1753–1758.
- [5] J. Chen, Z. Hu, and W. Chen, "Load prediction of integrated energy system based on combination of quadratic modal decomposition and deep bidirectional long short-term memory and multiple linear regression," *Autom. Elect. Power Syst.*, vol. 45, no. 13, pp. 85–94, Jul. 2021.
- [6] J. Shi, T. Tan, and J. Guo, "Multi-task learning based on deep architecture for various types of load forecasting in regional energy system integration," *Power Syst. Technol.s*, vol. 42, no. 412, pp. 25–34, 2018.
- [7] B. Chen and Y. Wang, "Short-term electric load forecasting of integrated energy system considering nonlinear synergy between different loads," *IEEE Access*, vol. 9, pp. 43562–43573, 2021.
- [8] M. Bozorg, A. Bracale, and P. Caramia, "Bayesian bootstrap quantile regression for probabilistic photovoltaic power forecasting," *Protect. Control Modern Power Syst.*, vol. 5, no. 3, pp. 36–47, 2020.
- [9] M. Madhiarasan, "Accurate prediction of different forecast horizons wind speed using a recursive radial basis function neural network," *Protect. Control Modern Power Syst.*, vol. 5, no. 3, pp. 48–56, 2020.
- [10] M. Q. Raza, N. Mithulanathan, J. Li, and K. Y. Lee, "Multivariate ensemble forecast framework for demand prediction of anomalous days," *IEEE Trans. Sustain. Energy*, vol. 11, no. 1, pp. 27–36, Jan. 2020.
- [11] H. Aprillia, H.-T. Yang, and C. Huang, "Statistical load forecasting using optimal quantile regression random forest and risk assessment index," *IEEE Trans. Smart Grid*, vol. 12, no. 2, pp. 1467–1480, Mar. 2021.
- [12] M. Tan, S. Yuan, S. Li, Y. Su, H. Li, and F. He, "Ultra-short-term industrial power demand forecasting using LSTM based hybrid ensemble learning," *IEEE Trans. Power Syst.*, vol. 35, no. 4, pp. 2937–2948, Jul. 2020.
- [13] J. Wang, J. Zhang, and X. Wang, "Bilateral LSTM: A two-dimensional long short-term memory model with multiply memory units for short-term cycle time forecasting in re-entrant manufacturing systems," *IEEE Trans. Ind. Informat.*, vol. 14, no. 2, pp. 748–758, Feb. 2018.
- [14] S. Siami-Namini, N. Tavakoli, and A. S. Namin, "The performance of LSTM and BiLSTM in forecasting time series," in *Proc. IEEE Int. Conf. Big Data (Big Data)*, Los Angeles, CA, USA, 2019, pp. 3285–3292.
- [15] Q. Li, T. Lin, S. Sun, S. Ke, and H. Du, "Critical clearing time prediction of power system fault based on machine learning," in *Proc. IEEE Sustain. Power Energy Conf. (iSPEC)*, Chengdu, China, 2020, pp. 2360–2365.
- [16] Y. Fan, S. Liu, L. Qin, H. Li, and H. Qiu, "A novel online estimation scheme for static voltage stability margin based on relationships exploration in a large data set," *IEEE Trans. Power Syst.*, vol. 30, no. 3, pp. 1380–1393, May 2015.
- [17] P. Zhou, P. Li, S. Zhao, and X. Wu, "Feature interaction for streaming feature selection," *IEEE Trans. Neural Netw. Learn. Syst.*, vol. 32, no. 10, pp. 4691–4702, Oct. 2021.
- [18] B. Shen and Z. Ge, "Weighted nonlinear dynamic system for deep extraction of nonlinear dynamic latent variables and industrial application," *IEEE Trans. Ind. Informat.*, vol. 17, no. 5, pp. 3090–3098, May 2021.
- [19] W. Pan, "Feature selection algorithm based on maximum information coefficient," in *Proc. 5th Adv. Inf. Technol. Electron. Autom. Control Conf. (IAEAC)*, Chongqing, China, 2021, pp. 2600–2603.
- [20] Z. Yue *et al.*, "Deep super-resolution network for rPPG information recovery and noncontact heart rate estimation," *IEEE Trans. Instrum. Meas.*, vol. 70, pp. 1–11, 2021.
- [21] H. Poostchi and M. Piccardi, "BiLSTM-SSVM: Training the BiLSTM with a structured hinge loss for named-entity recognition," *IEEE Trans. Big Data*, vol. 8, no. 1, pp. 203–212, Feb. 2022.
- [22] Z. Wu, Q. Li, and X. Xia, "Multi-time scale forecast of solar irradiance based on multi-task learning and echo state network approaches," *IEEE Trans. Ind. Informat.*, vol. 17, no. 1, pp. 300–310, Jan. 2021.
- [23] J.-B. Fiot and F. Dinuzzo, "Electricity demand forecasting by multi-task learning," *IEEE Trans. Smart Grid*, vol. 9, no. 2, pp. 544–551, Mar. 2018.
- [24] Z. Wang, Y. Wang, J. Zhang, C. Hu, Z. Yin, and Y. Song, "Spatial-temporal feature fusion neural network for EEG-based emotion recognition," *IEEE Trans. Instrum. Meas.*, vol. 71, pp. 1–12, 2022.
- [25] G. Sarah, *Introduction to Machine Learning with Python*. Newton, MA, USA: O'Reilly Media, 2017.
- [26] K. Chen, K. Chen, Q. Wang, Z. He, J. Hu, and J. He, "Short-term load forecasting with deep residual networks," *IEEE Trans. Smart Grid*, vol. 10, no. 4, pp. 3943–3952, Jul. 2019.
- [27] "AUS Campus Metabolism." May 1, 2021. [Online]. Available: <http://cm.asu.edu/>
- [28] "NSRDB Data Viewer." May 1, 2021. [Online]. Available: <https://maps.nrel.gov/nsrdb-viewer/>

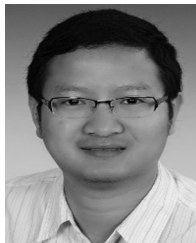
- [29] R. Malhotra and S. Meena, "Empirical validation of cross-version and 10-fold cross-validation for defect prediction," in *Proc. 2nd Int. Conf. Electron. Sustain. Commun. Syst. (ICESC)*, 2021, pp. 431–438.



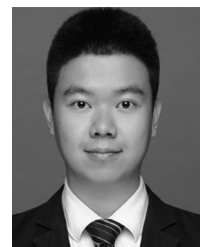
Xixiu Guo was born in Fujian, China, in 1995. She received the B.S. degree and the M.S. degree in electrical engineering from Hunan University, Changsha, China, in 2017 and 2020, respectively, where she is currently pursuing the Ph.D. degree with the College of Electrical and Information Engineering. Her research interests include data analytics in multiple energy system and smart grid.



Yujie Mei was born in Anhui, China, in 1998. He received the B.S. degree from Hunan University, Changsha, Hunan, China, in 2020, where he is currently pursuing the M.S. degree with the College of Electrical and Information Engineering. His research interest includes load forecasting in distribution network.



Yong Li (Senior Member, IEEE) was born in Henan, China, in 1982. He received the B.Sc. and Ph.D. degrees from the College of Electrical and Information Engineering, Hunan University, Changsha, China, in 2004 and 2011, respectively, and the second Ph.D. degree from the Institute of Energy Systems, Energy Efficiency, and Energy Economics, TU Dortmund University, Dortmund, Germany, in June 2012, where he has been working as a Research Associate since 2009. After that, he was a Research Fellow with The University of Queensland, Brisbane, Australia. Since 2014, he has been a Full Professor of Electrical Engineering with Hunan University. His current research interests include power system stability analysis and control, ac/dc energy conversion systems and equipment, analysis and control of power quality, and HVDC and FACTS technologies.



Jinjie Lin (Student Member, IEEE) was born in Fuzhou, Fujian, China, in 1995. He received the B.S. degree and the M.E. degree in electrical engineering from Hunan University, Changsha, Hunan, China, in 2018 and 2020, respectively, where he is currently pursuing the Ph.D. degree in electrical engineering with the College of Electrical and Information Engineering. His research interest is electric power optimization and control.



Xuebo Qiao (Student Member, IEEE) was born in Zhangjiakou, China, in 1992. He received the B.Sc. degree and the M.S. degree in electrical engineering from Hunan University, Changsha, China, in 2015 and 2018, respectively, where he is currently pursuing the Ph.D. degree. His research interests include active distribution networks planning and operation, and stochastic optimization in integrated energy systems.



Yicheng Zhou (Senior Member, IEEE) received the B.S. degree in civil engineering and the M.S. degree in mechanical engineering from Hunan University, China, in 1982 and 1986, respectively, and the Ph.D. degree in electrical engineering from Tokyo Metropolitan University in 1995. After working with TEPICO SYSTEMS and FUJITSU Limited, he is currently a Visiting Professor with Waseda University and a Chief Researcher with EETRI. His fields of interests include planning, operation, control, and optimization of electrical power systems.

He is a Senior member of IEEJ and a Project Leader of ISO 37153.



Zhenyu Zhang was born in Hebei, China, in 1994. He received the B.S. degree from Hunan University, Changsha, Hunan, China, in 2018, where he is currently pursuing the Ph.D. degree with the College of Electrical and Information Engineering. His research interests include nonintrusive load monitoring and data analytics in smart distribution networks.



Wangfeng Zhou was born in Zhejiang, China, in 1996. He received the B.S. degree and the M.S. degree in electrical engineering from Hunan University, Changsha, Hunan, China, in 2018 and 2021, respectively. His research interest is related to the smart grid.

Yosuke Nakanishi (Member, IEEE) received the B.S. and M.S. degrees in electrical engineering from Waseda University in 1978 and 1980, respectively, and the Ph.D. degree from Tokyo Metropolitan University in 1996. He joined Fuji Electric Company in 1980. After starting his career in research and development section, he has mainly dedicated himself to power system analysis work as well as the development of power system simulators and engineering programs for monitoring control systems. He is currently a Professor with the Graduate School of Environment and Energy Engineering, Waseda University. His research interests include simulation and analysis of power systems and distribution power systems. He received the Prize Paper Award from IEEE Power Engineering Education Committee in 1991. He is a Senior Member of the IEE of Japan and a member of CIGRE. He is also a Convenor of Investigation Committee on Grid Technologies for large amount of Wind Power, IEEJ, and a member of Investigation Committee on history of power system analysis, IEEJ.